# We are IntechOpen,
# the world's leading publisher of
# Open Access books
# Built by scientists, for scientists

## 6,900
Open access books available

## 186,000
International authors and editors

## 200M
Downloads

Our authors are among the

## 154
Countries delivered to

## TOP 1%
most cited scientists

## 12.2%
Contributors from top 500 universities

CLARIVATE ANALYTICS
**BOOK CITATION INDEX**
INDEXED

**WEB OF SCIENCE**™

Selection of our books indexed in the Book Citation Index
in Web of Science™ Core Collection (BKCI)

# Interested in publishing with us?
# Contact book.department@intechopen.com

Numbers displayed above are based on latest data collected.
For more information visit www.intechopen.com

# Synthesis and Characterization of Forsterite (Mg$_2$SiO$_4$) Nanomaterials of Dunite from Sumatera

*Ratnawulan Ratnawulan and Ahmad Fauzi*

## Abstract

The topics to be discussed are about the synthesis and characterization of forsterite nanoparticles (Mg$_2$So$_4$) from dunite rocks originating from West Sumatra. This region is a meeting of two Indian and Australian plates that give rise to mineral dunite with unique characteristics. Forsterite synthesis was carried out using calcinations temperature variations namely 700, 800, 900, 1000 and 1100°C. Synthesis of forsterite nanoparticles used the High Energy Milling Ellipse 3D Motion (HEM-E3D) method with variations in milling time, i.e., 5, 10, 20 h. Characterization was carried out using X-Ray Fluorescence (XRF) and X-Ray Diffraction (XRD) and Scanning Electron Microscopy (SEM). The synthesis results explain the forsterite concentration in dunite rock, pure forsterite at optimal calcinations temperature, forsterite nanoparticles at optimal grinding time and forsterite nanoparticle structure.

**Keywords:** forsterite, nanoparticles, dunite, HEM-E3D, milling time

## 1. Introduction

Forsterite is a magnesium silicate crystal with the chemical formula Mg$_2$SiO$_4$ derived from the olivine mineral group [1]. Olivine is a group of minerals composed of iron (Fe) and magnesium (Mg). The olivine mineral is green, with luster, formed at high temperatures. This mineral is commonly found in basalt and ultramafic rocks. Rocks whose overall minerals consist of olivine minerals are known as dunite rocks [2, 3].

Forsterite is often used as an electronic component because it has a low coefficient of thermal expansion and electrical conductivity [4]. Besides that, forsterite has superior properties, namely chemical stability at high temperatures [5] and high electrical properties so that it can be used as a coating for the back, edges, and front of iron and steel [6–11].

Iron and steel are widely used in industry and property such as building materials, ships, electronic equipment, etc. But in its use, steel is easily corrosion. To overcome this corrosion problem, a lot of research continues. One of them is by soaking the steel with an anti-corrosion solution. But the results are not yet suitable for achieving commercial applications. The reason is that the particle size of the anti-corrosion powder used is relatively very large, giving rise to new problems,

namely iron and steel which look uneven and homogeneous so that it disrupts appearance or esthetics.

Nanoparticle technology brings fresh air in an effort to increase the resistance of steel to corrosion. With a very small particle size, the problem can be solved. Nanoparticles are very fine so they are homogeneous. The use of nanoparticles is widely applied in various fields, including industrial fields such as paint, health, etc. Nanometer-sized materials have chemical and physical properties that are superior to large (bulk) material [12]. Nanoparticles have several advantages, namely having a larger touch surface area so that the bond between one particle and another is easy to form, and the mechanical, optical, and chemical properties of the material can experience significant differences with the properties of the sized material micrometer [13].

The advantage of forsterite made in nanometer size is that it is very strong, hard, and resilient at high temperatures, and is waterproof, corrosion resistant and has very active chemical properties that add durability when used for iron and steel coatings. Economical studies of nanoforsterite or nanomaterials are far more economical than conventional [14].

Forsterite nanoparticles can be made chemically and mechanically. Chemical methods are co-precipitation, solvothermal, sol-gel, solid state, and others. The mechanical method is by using a ball mill [15]. The advantage of using mechanical milling is a simple and effective method for growing solid crystals (the size of crystal grains becomes small) without going through chemical reactions that require a long time in the process of nanoparticle synthesis [15].

Forsterite nanoparticle synthesis has been carried out using synthetic samples with the milling method [16–18]. The crystallite and grain size obtained from the synthesis of nanoforsterite can be seen in **Table 1**.

**Table 1** shows the grain sizes of different forsterites resulting from several different research treatments. Size the forsterite nano single phase is formed after 40 h of milling and heating the temperature is 1000°C with a holding time of 1 h. The grain size of the Forster produced is a range between 0.1 and 2 µm [16]. The synthesis of forsterite nanoparticles was then continued using talc and magnesium oxide by the same method [17]. The variation in milling time is increased to 60 h with a heating temperature of 1200°C. The grain size obtained is less than 500 nm. Another study also uses a milling process with a variation of 5, 10, 20, and 30 h milling with temperature variations of 850–1100°C. Forsterite nanopowders were prepared from MgO and $SiO_2$ mixtures by using a high energy ball milling method. The results found that the average particle size was reduced to 147.4 nm [18].

| Methods | Ref. | Milling Time | Temperature (°C) | Crystalite Size (nm) | Grain Size |
|---|---|---|---|---|---|
| Milling | 16 | 5 min- 40 h | 1000 | 49 | 0.1 - 2 µm |
| Milling (continued using talc and magnesium oxide material) | 17 | 1 min-60 h | 1200 | 33 | < 500 nm |
| Milling | 18 | 5-30 h | 850-1100 | - | 147.4 nm |
| High Energy Milling | Current Chapter | 5-40 h | 26-1100 | 18.78 | 345 nm |

**Table 1.**
*The crystallite and grain size obtained from the synthesis of nanoforsterite.*

Characterization using XRD found that there was still Fe and Cr with a low content of 0.4256 and 0.5056%, respectively. Although many researchers have synthesized forsterite nanoparticles, the results obtained are still contaminated with other elements even at low levels. Contamination of samples with other elements can affect the nature of the final product.

This chapter discusses the synthesis and characterization of forsterite nanoparticles using High Energy Milling Ellipse 3D Motion (HEM-E3D). HEM-E3D is a unique technique that uses collision energy between crush balls and chamber walls which are rotated and moved in a certain way. The advantages of High Energy Milling is that in a relatively short time it can make nanoparticles (it takes several hours, depending on the type of tool), nanoparticles are produced in relatively large quantities. Besides that, the milling technique is one technique for growing solid crystals without going through the vaporation phase or chemical reaction treatment as is usually needed in the synthesis process in general.

## 2. West Sumatra and its geographical condition

The forsterite discussed in this chapter comes from dunite rocks originating from West Sumatra. West Sumatra is one of the regions in the Indonesian archipelago which has a fairly complex geological order. The West Sumatra region is traversed by the equator (zero degrees latitude), precisely located in the Bonjol subdistrict of Pasaman district, because of the influence of this location, West Sumatra has a trophic climate with high temperatures and humidity. The land surface height between one area and another area varies greatly. However, physically, West Sumatra is a region that is largely photographed by the mountains and the Bukit Barisan plateau which stretches from the North West to the Southeast, 63% and the area is a dense forest with elevations up to 3000 m above sea level.

The geographical condition of West Sumatra is quite unique which is partly located in the lowlands and partly in the highlands, marked there are many mountains, lakes, valleys/canyons, and rivers. This situation is due to its location at the confluence of three plates, namely the Eurasian plate to the north, the Australian Indian plate to the south and the Pacific plate to the east. The position of West Sumatra which is near the collision of two large plates namely the Australian Indian plate and the Eurasian Plate in addition to receiving negative consequences of natural disaster-prone areas also benefits, namely the emergence of sources of minerals containing economic minerals to the surface, one of which is dunite rock. **Figure 1** is dunite rock from West Sumatra.



**Figure 1.**
*Dunite rocks from West Sumatra.*

## 3. Dunite rock and its characteristics

Dunite is the main ingredient of the Earth's mantle and is rarely found in continental rock. Dunite is found when mantle rock plates from the subduction zone have been elevated to the continental crust. Dunite formation takes place in conditions that are dense or almost dense (at high temperatures) in a magma solution and before it cools to this temperature, the rock is ready to unite to form a binding anhedral olivine mass [19].

Dunite is a greenish-black rock and has a mineral composition almost entirely of monomineralic olivine (generally magnesia olivine) [20, 21]. Its mineral accessories include chromites, magnetite, limonite, and spinel. Olivine mineral is an iron-magnesium silicate with its chemical formula $(Mg, Fe)_2 (SiO_4)$, has an orthorhombic crystalline system, has no hemisphere, has a hardness of 6.5–7, specific gravity 3.27–4.37, has a gloss light, and the color of this mineral is yellowish green and grayish green. Olivine is one of the most common minerals on the surface of the earth and has also been identified on the surface of the Moon, Mars, and comets. Olivine minerals are generally as rock-forming minerals and also as accompanying minerals, in alkaline rocks such as gabbros, peridotite, etc. [21].

Dunite rocks naturally contain magnesium $(MgO)$ and have a very alkaline pH, which is around 7.5–9.5. These rocks can be used as basic fertilizer (natural) and compound fertilizer. $MgO$ is one of the most important elements for plants for photosynthesis, while the pH level of rocks can neutralize acid soils such as peatlands. Because the magnesium content of dunite rocks is quite high, the fertilizer with rock material will be very beneficial for agricultural and plantation activities.

Dunite contains 36–42% $MgO$ and 36–39% $SiO_2$. Olivine is a commercial source of a combination of magnesia and silica used in metallurgy. The content will increase if it is affected by an increase in temperature. The phase diagram of dunite consists of two phases namely forsterite and fayalite. The characteristics of the forsterite phase are melted at 1890°C and fayalite melts at a temperature of 1205°C [22]. Ultramafic frozen rock is an igneous rock which chemically contains less than 45% $SiO_2$ from its composition. The mineral content is dominated by heavy minerals with elements such as Fe (iron) and Mg (magnesium) which are also called ultramafic minerals [23]. The mineral composition and structural characteristics of dunite mainly contain olivine minerals and always contain little brucite, spinel-chromite, magnetite, and pyroxene. For comparison, dunites from South Turkey have chemical compositions such as FeO: 7.05%, $SiO_2$: 38.74%, MgO: 37.16%, CaO: 9.24%, $Al_2O_3$: 1.65% [24].

## 4. The olivine mineral

Olivine is the name of a group of rock-forming minerals found in mafic and ultramafic igneous rocks such as basalt, gabbro, dunite, diabas, and peridotite. Olivine is usually green and has a chemical composition ranging from $Mg_2SiO_4$ and $Fe_2SiO_4$. Olivine has a high crystallization temperature compared to other minerals. Olivine is the first mineral that crystallizes from magma. Olivine crystals are formed during the slow cooling process of magma and then settle in the bottom of the magma kitchen because of its relatively high density. This olivine accumulation can cause dunite-like rock formation at the bottom of the magma kitchen.

The minerals in the olivine group crystallize in the orthorhombic system (Pbnm space group) with silicates, which means that olivine is nesosilicate. In an alternative view, the atomic structure can be described as hexagonal, near oxygen ions with half of the octahedral atoms bonded to magnesium or iron ions and
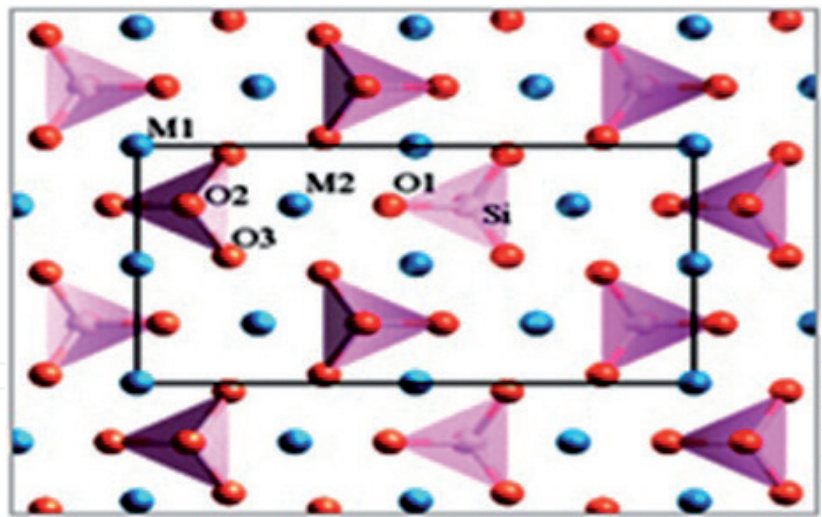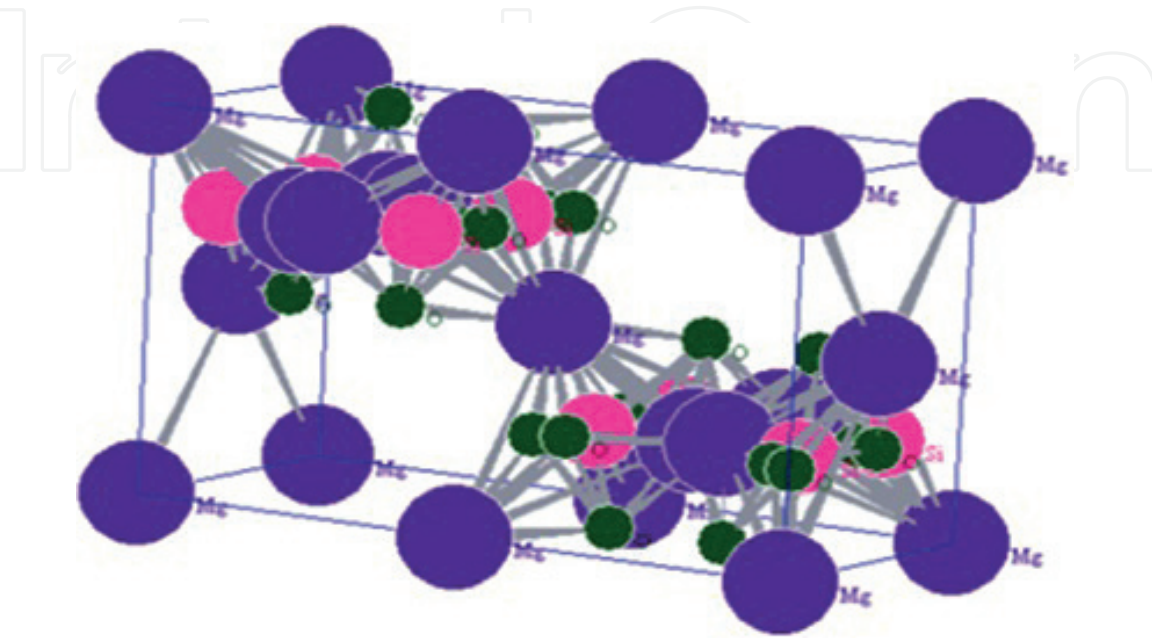
**Figure 2.**
*Crystal structure of olivine [12].*

one-eighth of tetrahedral occupied by silicon ions [12]. The shape of the olivine crystal structure can be seen in **Figure 2**.

## 5. Forsterite and its characteristics

Forsterite is a member of the olivine mineral prepared by Mg and Si. The general formula is $Mg_2SiO_4$. **Figure 3** shows the shape of the forsterite crystal structure.

**Figure 3**, Mg atoms are shown in purple, Mg2+ green, Si4+ white, and O2− pink. The radius of the Mg atom is 1.6 Å, Mg2+ is 0.75 Å, Si4+ is 0.4 Å, and O2 is 1.35 Å. A common characteristic of forsterite is the orthorhombic crystal system with the dimensions of cells a ≠ b ≠ c, where a = 4.79 Å; b = 10.19 Å; c = 5.85 Å with α = β = γ = 90° and space group Pbnm and density (g cm⁻³) is 3.275 [26].

Forsterite has a low electrical conductivity making it ideal for electronic materials. In addition, forsterite has a high melting point which is equal to 1890°C



**Figure 3.**
*Crystal structure of forsterite [25].*

which indicates that forsterite is a refractory material and ceramic manufacturing application because it has good chemical stability and a low coefficient of thermal expansion [27].

## 6. Nanoparticles technology

The nanoparticle technology is a material technology that deals with the creation or synthesis of small particles in nanometers (one per billion meters). The purpose of this technology is to use it for a more efficient future life. Nanoparticle synthesis can be done in two ways, namely top down and bottom up. Top down is the making of nanostructures by minimizing large material by mechanical activation, while bottom up is a way of assembling atoms or molecules and combining them through chemical reactions to form nanostructures. An example of a bottom up technology is using sol gel techniques, chemical precipitation, and phase agglomeration while top down method is grinding with a milling tool such as HEM-E3D [15].

The process that occurs during milling can be explained below. Mechanical milling is a simple and effective method for growing solid crystals (the size of crystal grains becomes smaller) without going through the evaporation phase or chemical reaction, as is usually needed in other synthesis processes [25]. This smoothing machine is able to convert hard and easily broken samples into powder-shaped analytical samples [14].

HEM-E3D is one tool used for mechanical alloys that use hard balls made of carbon steel. HEM-E3D vibrates samples with engine shocks because milling is used for a collision of kinetic energy in the sample. The speed of the media causes a high amount of energy to form to collide with the sample. Various combinations of media milling are used in HEM. A ratio of balls to powder, or BPR (Ball Powder Ratio), usually also used to change milling parameters [28].

HEM-E3D is very good for reducing particle size. The nature of particle size reduction and subsequent growth is the same as oxide analysis. In the milling process, HEM-E3D works by destroying the powder mixture through the mechanism of colliding milled balls that move to follow the movement pattern of the three-dimensional elliptical container that allows the formation of nanometer scale powder particles due to the high frequency of collisions. The high frequency of collisions that occur between the mixture of powder and milled balls is caused by the container rotating at high speed, which reaches 500 rpm, and the shape of the spherical movement of the three-dimensional ellipse.

Milling with ball mill is used for pulverizing the powder into nanoparticles because there is a grinding of powder on the surface of the ball when it collides with another ball so that the impact size given by the ball is as big as the collision force of the surface area of the ball. There are two collision paths where the material is between two balls and pulverization where the material is exposed to the ball when it is close to the cylinder wall. The interaction between the balls in the chamber is shown in **Figure 4**.

**Figure 4** shows the interaction between the balls in the chamber. The ball that has a smaller impact area, will give greater impact so that the destructive ability strengthens with the reduction of the touch area. Therefore, nanoparticle powder is easier to form by using smaller balls. Besides that, the collision frequency is the accelerating destruction factor.

The formation of forsterite nanoparticles using HEM-E3D will be more helpful because this tool has several advantages including machines that can be used can be used to do mixing, homogenization (uniformity), chemical mechanic (making chemical-mechanical reactions), mechanical milling, mechanical alloys, and do an
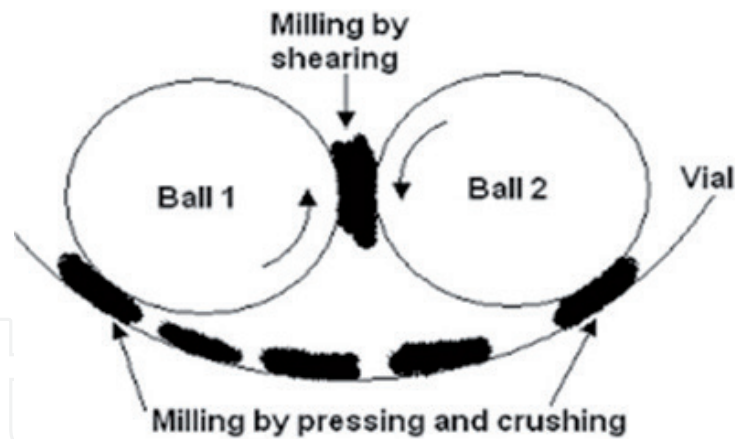
**Figure 4.**
*Interaction between grinding balls in high energy milling [29].*

emulsion. So nanoparticles will be produced by smoothing the material up to the nanometer scale, high destruction rate, easy conditioning of the milling system so that the mechanism of amorphization and nanoparticle formation process is faster and more effective, becoming a tool for making nanopowder at low prices and increasing efficiency and electronic systems integrated system includes a motor controller, and a timer.

Process parameters that must be considered in the grinding process include speed and time of grinding, comparison of ball weight to weight of powder, and empty space in the grinding container. In simple terms, increasing the rotation speed of the milling will increase the energy input to the powder. How fast the rotation of milling is affected by the design of the instrument. Speed also affects the increase in the temperature of the media milling. If the grinding speed is too high, the temperature of the components in the grinding process will increase. This increase in temperature can be advantageous for example when diffusion is needed to produce homogenizes and fusion of powder. The disadvantage is excessive friction or collision of the milling equipment that carries contamination.

The rotation speed used is adjusted so that the milling process runs optimally. If the rotation speed is set too fast, the balls will only rotate on the cylinder wall due to centrifugal force. Conversely, when the rotation speed is very low, the impact energy to destroy the material is not enough so that the process will last long.

The milling time needed also depends on the type of milling used, intensity of milling, ball-powder ratio, and milling temperature. Long milling times from the time needed will increase contamination and some unwanted phases will be formed. Therefore, milling powder did not require a long time for sample preparation.

In addition, the size of the ball greatly affects the efficiency of milling, where generally large ball sizes (with high density) are more useful because greater weight can transfer greater impact and kinetic energy to powder particles. While small balls produce more friction, making it easier to form an amorphous phase. The resulting grain size is also smaller when the ball used is small. In practice, a combination of various sizes is often used. The use of the same size of balls can cause the ball to rotate along the bullet path and not hit the surface of the powder randomly. The larger the size of the ball used, the greater the energy when pounding, but when the material is small, the collision will rarely occur because space, where the collision occurs, becomes smaller and in the end, the process will not be optimal.

For small scale or laboratory, generally, the ratio of balls to the weight of powder used is around 10:1, 10 g of balls and 1 g of powder, while for large scale
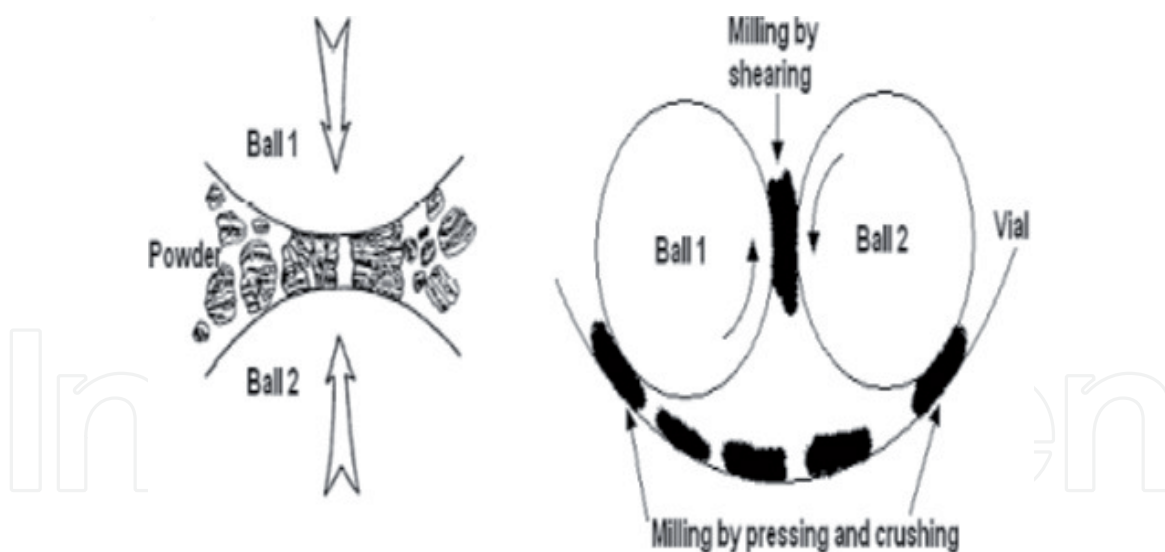
**Figure 5.**
*Concept of powder destruction at ball mill [29].*

or industrial scale, the ratio of ball weight to the weight of powder used can reach 100:1. The higher the ratio of the weight of the ball to the weight of the powder used, the shorter the frequency of impact.

The grinding procedure is a forsterite powder inserted into a metal chamber with several steel balls in it that move continuously. The size of the milled ball used in this process is a small milled ball with a diameter of 5 mm with a weight of 0.5 g. The ratio of the weight of the milled ball to the weight of the powder in the grinding container used is 10:1. For example, the weight of the milled ball is 150 g while the amount of powder is 15 g. In the metal chamber, the balls will collide with each other. As a result of this ball collision, the homogeneous powder that is inserted into this tool will be crushed between the balls. This causes the particles to break. And so on until it reaches the desired size [30]. **Figure 5** shows the concept of destruction of sample powder in the ball mill.

## 7. Synthesis of nanoparticles from forsterite

The synthesis of nanoparticles from forsterite discussed here comes from dunite rock samples taken from the West Sumatra region, precisely at coordinates: 00° 09′ 01.1″ LU and 99° 53′ 19.5″ BT. Samples were sieved with 2.1 mm sieves to obtain finer and homogeneous samples. The sample was then crushed for 3 min using bowl mill so that the samples were finer and homogeneous. Samples were tested by X-Ray Fluorescence (XRF) to see the composition of the compounds in the dunite. The results of XRF are known to dunite rocks found in West Sumatra, Indonesia has a composition of FeO: 11.12%, $SiO_2$: 31.18%, MgO: 49.96%, CaO: 7.31%, $Al_2O_3$: 0.43%. MgO content in this region is quite high when compared to Southern Turkey [24]. To get forsterite minerals from dunite samples, calcination was carried out with temperature variations of 700, 800, 900, 1000, and 1100°C. Then the samples were carried out X-Ray Diffraction (XRD) test to see the phases which appear for each calcination temperature. From the results of XRD, it is known that the forsterite phase at the optimum calcination temperature.

Samples with optimum calcination temperature are then taken to be further synthesized into forsterite nanoparticles. Samples were weighed as much as 2 g and milling balls as much as 20 g for each milling time. The type of milling ball used is small carbon steel with 40 pieces which weigh 0.2 per fruit. Medium sized milling

balls of 4 which weigh 0.5 per piece. While large milling balls as much as two pieces weighing 3.55 g per fruit. The samples that have been prepared are then processed using HEM-E3D with variations in milling time of 5, 10, 20, 40, and 60 h. The length of the milling process in each cycle is carried out for 30 seconds, and then the process is stopped for 1 min to avoid an increase in temperature and damage to the milling device due to rising motor temperatures that are too high.

## 8. Calcination and the effect of calcination temperature on the raw material structure

The characterization of forsterite nanoparticles was carried out using X-ray Diffraction (XRD) and Scanning electron microscopes (SEM). XRD is used to determine the structure and size of crystals of forsterite for each variation of milling time. The crystal size of forsterite is calculated using the Scherrer formula, $D = 0.9\,\lambda/\beta\cos\theta$, where $\lambda$ was the wavelength of X-ray radiation, $\beta$ was the full width at half maximum (FWHM) of the peaks at the diffracting angle $\theta$ [31]. SEM is used to see the microstructure or morphology of forsterite and particle size. The results of the XRD test from dunite raw material for each calcination temperature variation can be seen in **Table 2**.

**Table 1** shows the appearance of the forsterite phase starting at the calcination temperature of 700°C. But at this temperature, other phases are still found, namely fayalite, lizardite, magnesium iron silicate, olivine and enstatite. For the synthesis of forsterite into nanoparticles, the sample taken is the result of calcination at a temperature of 1100°C. The reason for taking this condition is the forsterite phase, even though the olivine phase is still found. Through the HEM-E3D method with variations in milling time, it is expected that the olivine phase can decompose into forsterite.

The XRD results for forsterite that have been milled for 5 h are shown in **Figure 6**.

**Figure 6** is a plot of the 2θ diffraction angle on the intensity of the XRD pattern of forsterite after being processed for 5 h. The figure shows that the sample is

| Calcinations' temperature (°C) | Phase | Structure | | | | |
|---|---|---|---|---|---|---|
| | | A(Å) | B | C | Space Grup | Crystal System |
| 26 | Lizardite | 5.31 | 5.31 | 7.31 | P31mE | Hexagon |
| | Magnetit | 8.39 | 8.39 | 8.39 | Fd-3m | Cubic |
| 700 | Fayalite | 4.76 | 10.23 | 5.99 | Pbnm | Orthorhom |
| | Forsterite | 5.98 | 10.19 | 4.76 | Pmnb | Orthorhom |
| 800 | Forsterite | 4.76 | 10.21 | 5.99 | Pbnm | Orthorhom |
| | Olivine | 10.19 | 5.98 | 9.51 | P1 | Anorthi |
| | Lizardite | 5.34 | 5.34 | 7.10 | P31m | Hexagon |
| 900 | Forsterit | 4.76 | 10.20 | 5.99 | Pbnm | Orthorhom |
| | Magnesium Iron Silicate | 4.76 | 10.22 | 5.99 | Pbnm | Orthorhom |
| 1000 | Forsterit | 4.76 | 10.21 | 5.98 | Pbnm | Orthorhom |
| | Olivine | 10.19 | 5.98 | 9.51 | P1 | Anorthi |
| | Enstatite | 18.23 | 8.81 | 5.17 | Pbca | Orthorhom |
| 1100 | Forsterite | 4.75 | 10.19 | 5.98 | Pbnm | Orthorhom |
| | Olivine | 10.19 | 5.98 | 9.51 | P1 | Anorthi |

**Table 2.**
*Structure of dunite raw material for each temperature variation of calcination.*
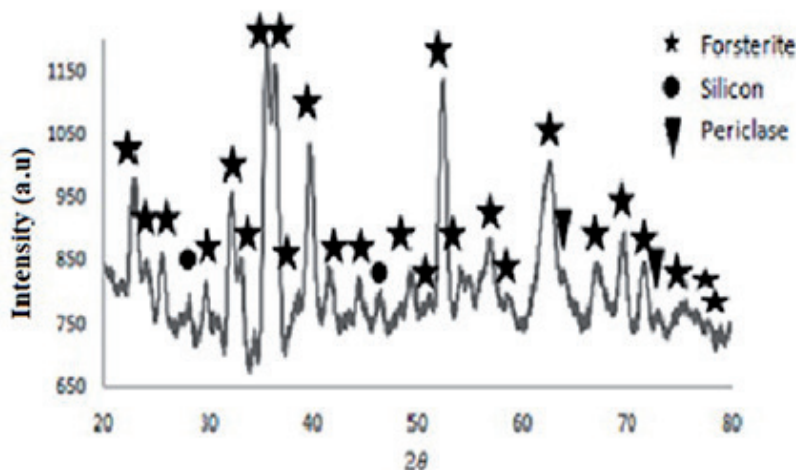
**Figure 6.**
*XRD pattern from forsterite after being milled for 5 h.*
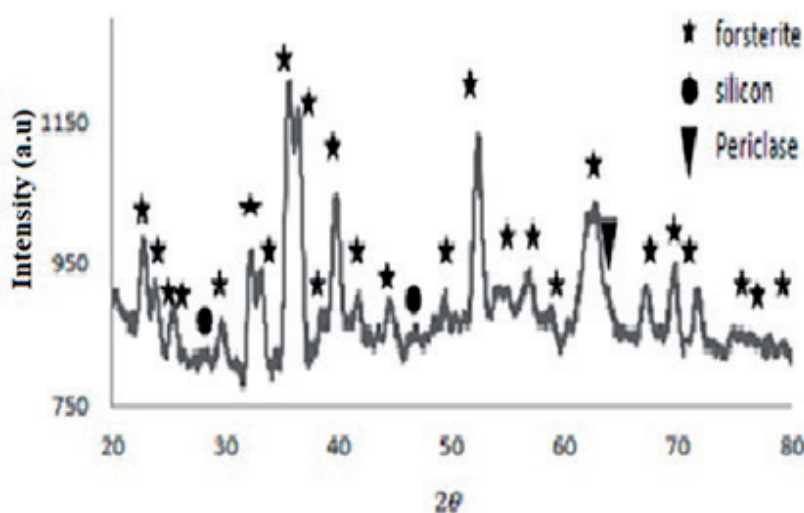


**Figure 7.**
*XRD pattern from forsterite after being milled for 10 h.*

dominated by the forsterite phase even though there are still other phases such as silicon which appear at scattering angles 2θ which are 26.63 and 47.2, and periclase with a scattering angle of 74.74 with a small degree.

Furthermore, for samples milled for 10 h, the XRD pattern is shown in **Figure 7**.

**Figure 7** shows the sample is still contaminated with phases other than forsterite. Forsterite milled for 10 h there are several phases, namely forsterite, periclase, and silicon, but the phase concentration of the Periclase begins to decrease compared to samples which are milled for 5 h. The dominant phase is still forsterite.

Furthermore, for samples milled for 20 h, the XRD pattern is shown in **Figure 8**.

**Figure 8** shows the sample is still contaminated with other phases other than forsterite. Forsterite milling for 20 h there are several phases, namely forsterite, periclase, and silicon. The dominant phase is still forsterite.

Furthermore, for samples milled for 40 h, the XRD pattern is shown in **Figure 9**.

**Figure 9** shows no other phases such as periclase, and silicon that appear other than forsterite phase. This result is achieved after the sample has been milled for 40 h.

Based on XRD data analysis for each sample, it can be seen that variations in milling affect the phase of the sample. The phase that appears after being given the influence of milling variations for 5, 10, 20, and 40 h is shown in **Figure 10**.
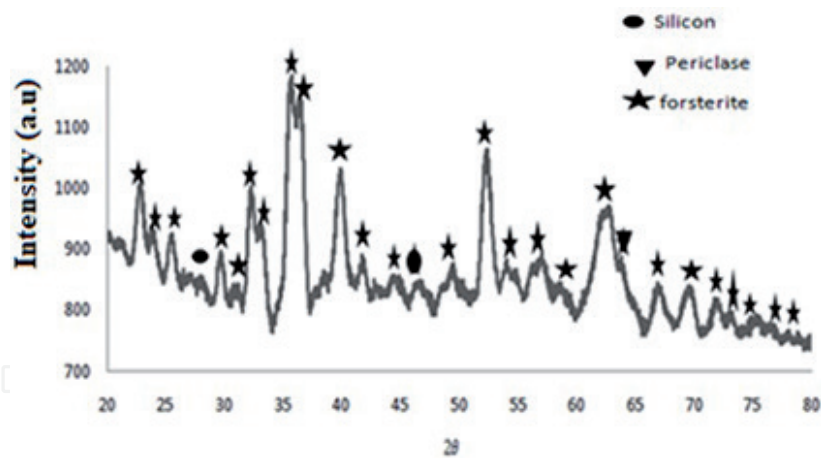
**Figure 8.**
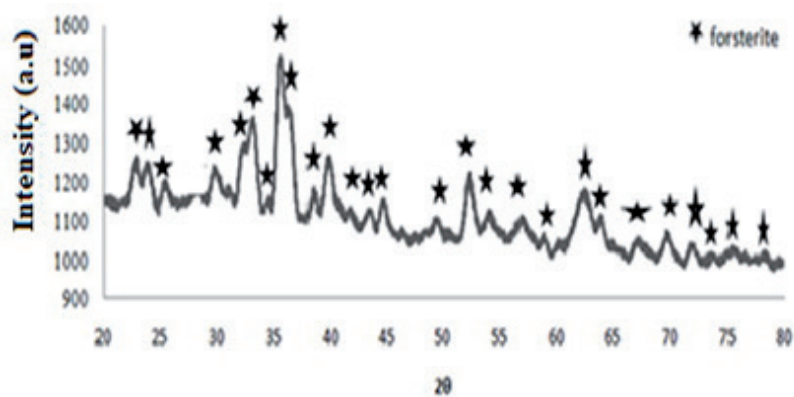*XRD pattern of forsterite after being milled for 20 h.*



**Figure 9.**
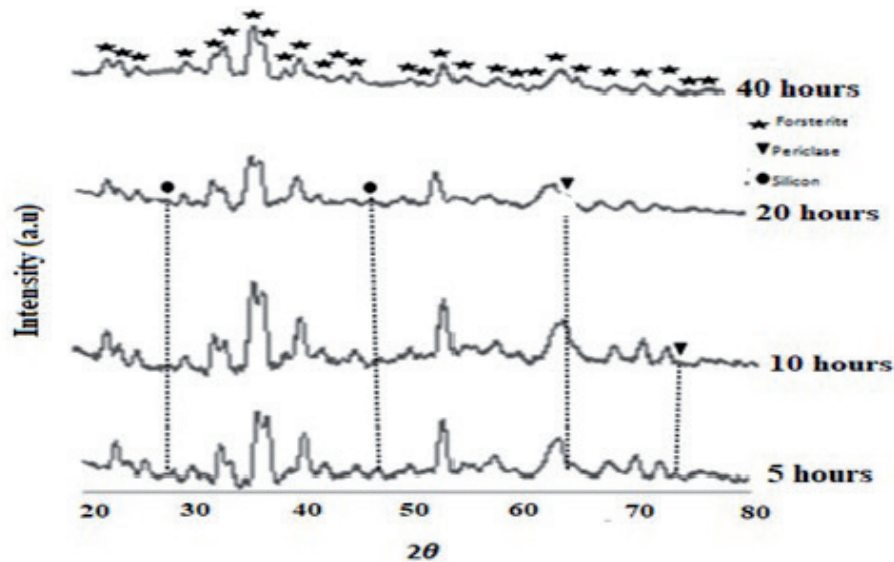*XRD pattern from forsterite after being milled for 40 h.*



**Figure 10.**
*Effect of milling time variation 5, 10, 20, and 40 h on the diffraction pattern of XRD results.*

**Figure 10** shows that at 5 h milling time, phases that appear forsterite, silicon, and periclase. The crystalline system at 5 h milling time is orthorhombic for the phosphoresce and cubic phases for the silicon and periclase phase. The crystallite size for the forsterite phase is 53.80 nm. While at the time of milling 10 h there was a clumping of grain size, so that the size of the crystallite became large i.e. 54.58 nm.

Phases that appear at 10 h milling time are forsterite, silicon, and periclase. Crystalline size at 20 h milling time is 21.69 nm. While at the time of 40 h milling, the size of the crystallite is getting smaller to 18.78 nm. Changes in crystal size to milling time can be seen in **Figure 11**.
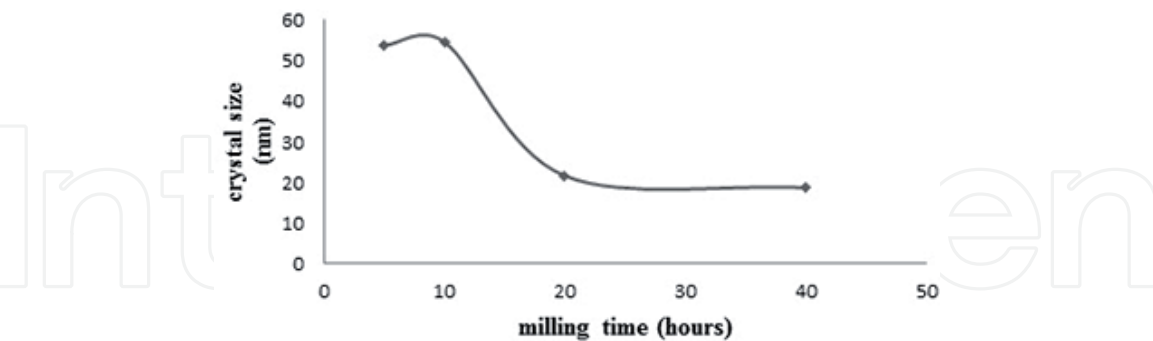


**Figure 11.**
*Effect of milling time on crystal size.*
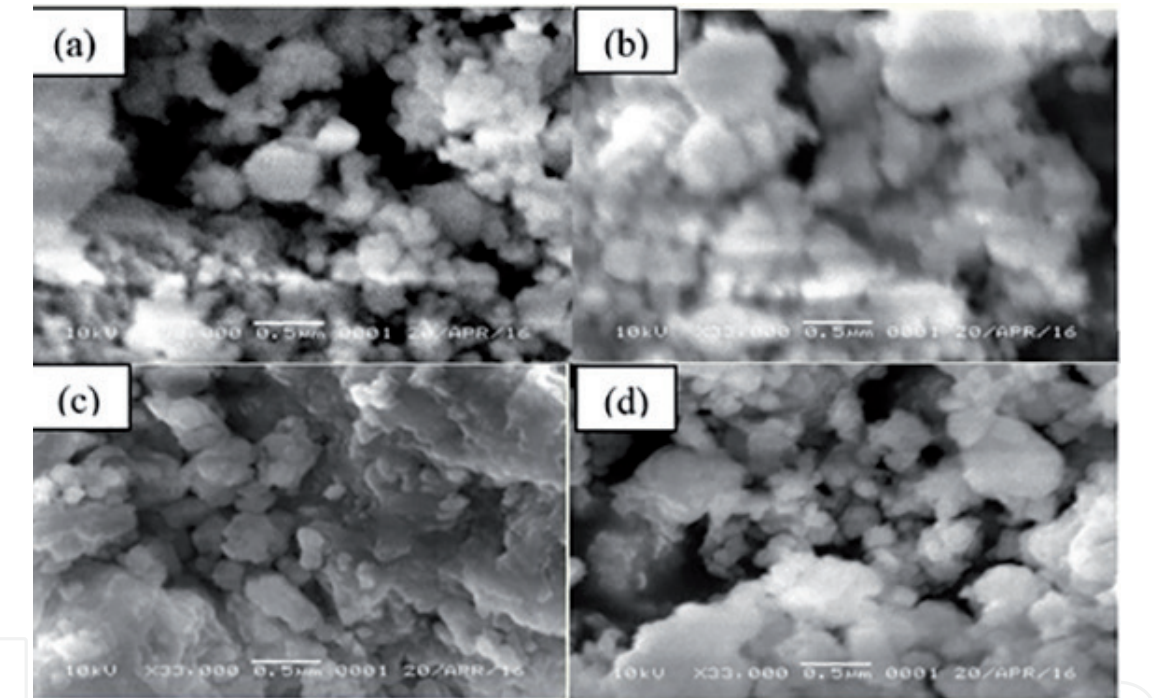


**Figure 12.**
*Differences in the form of morphology in each milling time variation with a magnification of 33,000×. (a) 5 h, (b) 10 h, (c) 20 h, (d) 40 h.*
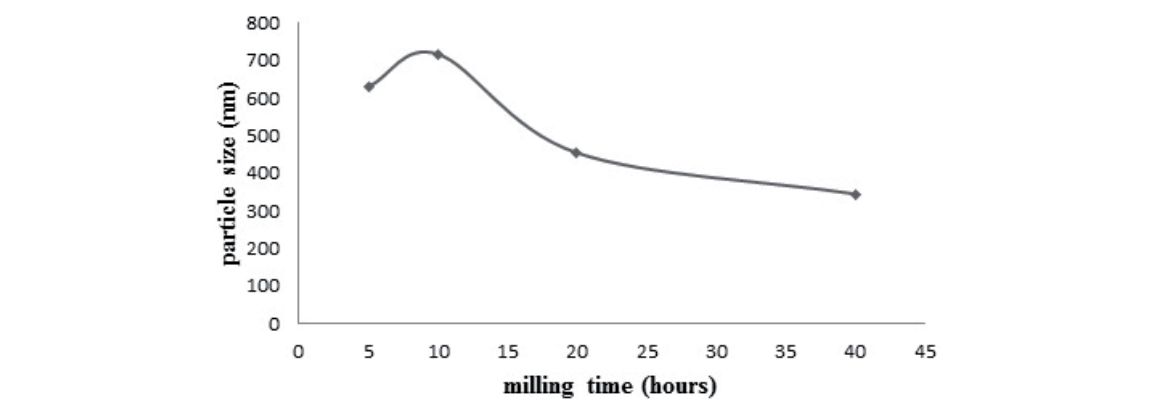


**Figure 13.**
*Effect of milling time on grain size.*

The milling time is very influential on the surface morphology of the sample, where the longer the process of milling is done, the smaller the particle size. **Figure 12** shows the morphology of forsterite powder with a variation of 5 h milling time. 10, 20 and 40 h were taken using SEM.

In **Figure 12**, there are differences in the form of forsterite morphology at each variation of milling time. At 5 h milling, the shape of the particles is round but not evenly distributed. Whereas at 10 h the particles clot back causing a large particle size. At 20 h the particle shrinks from the particle size to milling time of 10 h. The shape of the particles has seen a little round shape but has not been flat. At the time of milling 40 h the particle size has decreased and there are already smaller particles than before but the particles are not evenly sized. The grain size of forsterite particles for variations of milling time (a) 5 h, (b) 10 h, (c) 20 h, (d) 40 h are respectively 630, 717, 454, and 345 nm. The graph of changes in grain size to milling time can be seen in **Figure 13**.

## 9. High-energy milling methods, and the effect of the different parameters

The milling time parameter does not affect the crystal structure of forsterite, but it affects the appearance of other phases with different crystal structures. HEM-E3D is used for mechanical activation in samples using a speed of 500 rpm so that collisions occur between milling balls so as to produce energy. The impact energy is used to stretch or break the bonds of atoms in the sample. The longer the grinding time, the higher the temperature on the collision of the milling balls. In the process, the faster the ball mill rotation, the greater the energy produced and produces higher temperatures [29].

High temperatures benefit in some cases that require a diffusion process to support the integration process in the powder and reduce internal stress or even eliminate it. However, in some cases, the temperature increase is very detrimental because it can produce an unstable phase so that it will form other structures during the milling process and the powder size will be larger. At high temperatures, the crystal structure can grow quickly, but more defects in the crystals formed. The lattice parameters of the crystal will also change due to crystal defects by the collision. The material that has been heated is then cooled slowly so that the atoms in the material can be arranged regularly to occupy the lattices to form a crystal. At certain times there will be a phase change.

The number of crystalline phases has quite a combination of atoms or groups of atoms. The amorphous phase is relatively small because it does not have a long-range order and the atomic arrangement is not clear. The phase difference that occurs is inseparable from the influence of energy possessed by atoms for the diffusion process. At a certain level of energy, atoms can stay away from each other. If an atom has enough energy to break its bonds a diffusion process will occur [32].

Mechanical activation is related to the formation of material which causes strain on the solid mixture. This is one form of mechanical alloying, involving two constituent powders with heterogeneous size distributions that will affect the material properties and mechanism of phase formation of a material. The process looks simple, where different types of metals can bind through exchanging short distances between atoms called atomic diffusion, this can happen if atoms have enough energy to release bonds with the surrounding atoms so that they can move from the original lattice position to the empty lattice position [33].

The explanation of the reduction in crystal size due to the increase in milling time is that during the milling process of powder samples with variations in milling

time there are four forces that occur in the material, namely impact (attrition), friction (shear), and compression (compression). With these four forces, the powder can be destroyed by a milling device in the formation of powder into nanoparticles. The size of the powder that has been crushed with a milling device becomes smaller than the size of the original powder.

The results of characterization using XRD obtained a relationship of 2θ with intensity. Every variation in the milling time shows that peaks appear and disappear and also the intensity decreases. The peak that disappears is because atoms in other phases do not exist so there is no scattering of atoms by certain structures. The measured intensity at XRD is the result of scattering intensity by certain atomic structures. The magnitude of the relative intensity of the series of peaks depends on the number of atoms or ions present and the distribution in the unit cell of the material. The decrease in intensity is due to changes in the size of the crystal, this change also causes the crystal structure of the forming element to change. The crystal size obtained when the 40-h milling time is 18.78 nm. For comparison the size of forsterite crystals obtained from talc $(Mg_3Si_4)_{10}(OH)_2$ and magnesium carbonate $(MgCO_3)$ material is 33 nm [17].

When milling can measure the crystal grain size of the sample. This is because, during the milling process, the powder particles will experience repeated processes of destruction. When the milling balls collide with each other, the powder milled is between the collisions of the balls so that the powder will deform and the powder will disintegrate which will cause the grain size to be small and can also cause it to become large if the grain has clotted.

Compressive forces (compaction) that occur in particles other than destroying or breaking particles can also damage the pores on the surface of the particles, the pores are damaged due to the compressive force, especially small diameter pores that are very vulnerable to damage and disappear. In mills that are too long, particles can undergo agglomeration. After a long grinding and with very fine particles, the coupling forces become larger, and the presence of chemical bonds or Van Der Waals forces with bond strengths of 40–400 kJ/mol can make particles fuse or agglomerate. Or if there are particles trapped and then given an impact force, the particles can also be agglomerated. With the finer particles due to the long grinding time, the distance between particles will be smaller and more contact between particles will allow agglomeration to occur. Thus, on particles with porous surfaces, agglomeration allows for the formation of enlarged pore diameters due to "pore merging" due to agglomeration between particles.

Thus it can be explained by the increasing milling time used, the grain size of powder particles will be smaller. This is what allows the formation of nanometer scale powder particles due to the high collision frequency and the length of time the milling is used.

The grain size at the time of 10 h milling is 717 nm, there is a little clumping at 10 h milling time, while at 5 h 630 nm, when processed in 20 h the grain size decreases to 454 nm, at the time of milling 40 h the size of the crystal again decreased to 345 nm. The size of the grain increases during the milling time of 10 h because the particles agglomerate again after the particles are broken or broken by balls so that they are small and then group up to the milling time for 10 h this occurs due to the powder that has been solved and has a small effect. Unified powder causes large grain size, but at 20 h milling the grain size shrinks again because the sample experiences collision forces with balls that have high energy so the powder becomes eroded again and becomes small in size. In addition to the impact force, the powder also experiences other styles such as attrition, friction, and compression. So that at the time of milling 20 h forsterite has reached the fracture point and its size shrinks again.

The milling time also affects the sample morphology. Each milling variation will produce different morphological forms. The collision between the milling balls and the powder repeatedly over time increases the milling time will make the particle size of the powder will be smaller. The SEM results also show that the grain size is getting smoother as the milling time increases. This happens because in HEM-E3D there are collisions of milling balls with powder. Assault particles are trapped between steel balls that are colliding. Furthermore, powders undergo microscopic deformation and fracture processes (breaking) and welding (joining).

The forsterite particle size of the West Sumatra dunite has a grain size of 345 nm. The size obtained has not reached below 100 nm. The milling process carried out shows that forsterite powder has a tendency to agglomerate or clump, thus making forsterite under 100 nm not yet reached. This is due to the ratio of the ball to the powder used and also the speed of milling, and the length of time the milling is used. The higher the ball mill rotational speed will increase the collision and fineness of the powder, but if the speed has reached a certain level the fineness of the powder decreases. Likewise with the ratio of the weight of the milling ball to the powder, the variation in the number of pounding balls will also increase the collision contact area of the pounding and powder balls.

The difference in forsterite morphology is also seen in every variation of milling time, this is because the granules have clumped between the grains with each other, and the shape of the granules is round and uneven. Each increase in the variable milling time looks more like the morphology of the mixture, it appears that between the grains with each other have merged with each other, and the fusion indicates the formation of a solid solution on the powder. The increase in grain size in one of the milling results is due to the agglomeration process. The agglomeration process is the process of joining small particles into a larger structure through a physical binding mechanism.

The agglomeration process that occurs can also be caused by several things, namely sample powder contamination with crushing ball material and jar. Even though it has very high hardness, stainless steel on the crushing ball and jar will still give contamination to the ground powder sample. The high grinding speed and long grinding time cause contamination of the forming material of the crushing ball and the jar can be said to be almost unavoidable. Furthermore, which affects the grain size, namely the effect of the jar shape, the bottom edge design of HEM-E3D jar in the form of a curve can cause the formation of a dead zone which is an area where the powder is not grounded because the grinding media cannot reach it during milling.

## 10. Conclusions

In summary, has been described the synthesis and characterization of nanoparticles from forsterite ($Mg_2SiO_4$) sourced from dunite rocks in West Sumatra. Forsterite is obtained from dunite powder by giving calcination temperature. HEM-E3D is used to obtain nanoparticles from forsterite. The results show that milling time affects crystal size, grain size and morphology of forsterite. The higher the milling time, the smaller the particle size of forsterite. The forsterite particle size obtained has not reached below 100 nm. However, this result is better than previous research using the same method. This is because forsterite powder has a tendency for agglomeration.

## Acknowledgements

## Author details

Ratnawulan Ratnawulan* and Ahmad Fauzi
Padang State University, Padang, Indonesia

*Address all correspondence to: ratnawulan@fmipa.unp.ac.id

**IntechOpen**

## References

[1] Cooper R, Halle P. Reaction between synthetic mica and simple oxide compounds with application to oxidation resistant ceramic composites. Journal of the American Ceramic Society. 1993;**76**(5):1265-1273

[2] Sarimai S, Ratnawulan R, Ramli R, Fauzi A. Effect of milling time on particle size of forsterite (Mg$_2$SiO$_4$) from South Solok district. In: IOP Conference Series: Materials Science and Engineering. Vol. 335; Padang, Indonesia; 2018

[3] Thornhill M. Dry magnetic separation of olivine sand. In: Physicochemical Problems of Mineral Processing. Norway: Norwegian University of Science and Technology; 2011

[4] Rani AB, Annamalai AR, Majhi MR, Kumar AH. Synthesis and characterization of forsterite refractory by doping with kaolin. International Journal of ChemTech Research. 2014;**6**(2):1390-1397

[5] Saberi A, Alinejad B, Negahdari Z, Kazemi F, Almasi A. A novel method to low temperature synthesis of nanocrystalline forsterite. Materials Research Bulletin. 2007;**42**(4):666-673. DOI: 10.1016/j.materresbull.2006.07.020

[6] Mostafavi K, Ghahari M, Baghshashi S, Arabi AM. Synthesis of Mg$_2$SiO$_4$:Eu$^{3+}$ by combustion method and investigating its luminescence properties. Journal of Alloys and Compounds. 2013:**555**:62-67

[7] Mehta NS, Majhi MR. Effect of sintering at different temperature to enhance the physical and mechanical properties of forsterite refractories doped with kaolin. International Journal of Innovative Research in Science, Engineering and Technology.

2016;**5**(9):16261-16266. DOI: 10.15680/IJIRSET.2016.0509086

[8] Pawley R. The reaction talc+forsterite=enstatite +H$_2$O; new experimental results and petrological implications. American Mineralogist. 1998;**83**(1):51-57. DOI: 10.2138/am-1998-0105

[9] Aranovich L, Newton R. Experimental determination of CO2–H2O activity-composition relations at 600-1000°C and 6-14 k bar by reversed decarbonation and dehydration reactions. American Mineralogist. 1999;**84**(9):1319-1332. DOI: 10.2138/am-1999-0908

[10] Maliavski N, Dushkin O, Markina J. Forsterite powder prepared from water soluble hybrid precursor. AICHE Journal. 1997;**43**(11A):2832-2836. DOI: 10.1002/aic.690431301

[11] Shieh Y, Rawlings R, West D. Constitution of laser melted alumina-magnesia-silica ceramics. Materials Science and Technology. 1995;**11**(9):863-869. DOI: 10.1179/mst.1995.11.9.863

[12] Jeevanandam J, Barhoum A, Chan YS, Dufresne A, Michael K, Danquah MK. Review on nanoparticles and nanostructured materials: History, sources, toxicity and regulations. Beilstein Journal of Nanotechnology. 2018;**9**:1050-1074. DOI: 10.3762/bjnano.9.98

[13] Bell TE. Understanding Risk Assesment of Nanotechology. USA: Artikel National Nanotechnology Coordination Office; 2006

[14] Kishore K. Study on the effect of high energy ball milling (a nano material process) on the microstructure and mechanical properties of a (Al-Si-Fe-Cu) alloy [Thesis]. Rourkela: National Institute of Technology; 2007

[15] CSSR K. Nanofabrication Towards Biomedical Applications. Weinheim, Germany: Wiley-VCH Verlag GmbH & Co. KGaA; 2005

[16] Tavangarian R, Emadi R. Mechanical activation assisted synthesis of pure nanocrystalline forsterite powder. Journal of Alloys and Compounds. 2009;**485**(1-2):648-652

[17] Tavangarian R, Emadi R. Mechanochemical synthesis of single phase nanocrystalline forterite powder. International Journal of Modern Physics B. 2010;**24**(3):343-350

[18] Cheng L, Liu P, Chen XM, Niu WC, Yao GG, Liu C, et al. Fabrication of nanopowders by high energy ball milling and low temperature sintering of $Mg_2SiO_4$ microwave dielectrics. Journal of Alloys and Compounds. 2012;**513**:373-377. DOI: 10.1016/j.jallcom.2011.10.051

[19] Koukouzasa N, Gemeni V, Ziock HJ. Sequestration of CO2 in magnesium silicates, in Western Macedonia, Greece. International Journal of Mineral Processing. 2009;**93**(2):179-186. DOI: 10.1016/j.minpro.2009.07.013

[20] Abdel-Karim AAM, Elwan WI, Helmy H, El-Shafey SA. Spinels, Fe-Ti oxide minerals, apatites, and carbonates hosted in the ophiolites of Eastern Desert of Egypt: Mineralogy and chemical aspects. Arabian Journal of Geosciences. 2014;**7**(2):693-709. DOI: 10.1007/s12517-013-0854-0

[21] Mohanty JK. Characterization of high magnesian rocks for suitability as flux in iron and steel industry. Journal of Geology and Mining Research. 2009, 2009;**1**(7):149-155. DOI: 10.5897/JGMR

[22] Nelson A. Silicate structures, structural formula, neso-, cyclo-, and soro-silicates. In: Mineralogy. New Orleans: Louisiana Tulane University; 2012

[23] Perepelitsyn VA, Kuz'menko NG, Kuperman YE, Visloguzova EA. The mineral composition of the dunites from the Solov'evogory deposits. Refractories. 1974;**15**(1-2):92-97. DOI: 10.1007/BF01286316

[24] Didem A. Petrogenesis of subduction zone and dunite bodies. International Journal of Earth Sciences and Engineering. 2012;**2**:377-386

[25] Quinn AW. Dana's manual of mineralogy (Hurlbut, Jr.; Cornelius S.). Journal of Chemical Education. 1952;**29**(10):532. DOI: 10.1021/ed029p532.2

[26] Ray W, Kent RW, Simon P, Kelley SP, Malcolm S, Pringle MS. Mineralogy and 40Ar/39Ar geochronology of orangeites (group II kimberlites) from the Damodar Valley, Eastern India. Mineralogical Magazine. 1998;**62**(3):313 323. DOI: 10.1180/002646198547701

[27] Kosanovic C. Synthesis of forsterite powder from zeolite precursors. Croatica Chemica Acta. 2005, 2005;**2**(79):203-208

[28] Decastro C, Mitchell B. Nanoparticles from mechanical attrition. In: Baraton M, Valencia CA, editors. Synthesis, Functionalization and Surface Treatment of Nanoparticles. Valencia: American Scientific Publishers; 2002. pp. 1-15

[29] Calka A, Nikolov JI. The dynamics of magneto-ball milling and its effects on phase transformations during mechanical alloying. Materials Science Forum. 1995;**179-181**:333-338. DOI: 10.4028/www.scientific.net/MSF.179-181.333

[30] Ozkaya T, Toprak MS, Baykal MSA, Kavas AH, Koseoglu HY, Aktas B. Synthesis of $Fe_3O_4$ nanoparticles at 1000C and its magnetic characterization. Journal of

Alloys and Compounds. 2008;**472**:18-23.
DOI: 10.1016/j/jallcom.2008.04.101

[31] Riazian M, Bahari A. Structure
of lattice strain and effect of sol
concentration on the characterization
of TiO$_2$-CuO-SiO$_2$ nanoparticles.
International Journal of Nano
Dimension. 2012;**3**(2):127-139

[32] Van V. Elements of Materials Science
and Engineering. Publication Reading,
MA: Addison-Wesley; 1989

[33] Eckert J, Holzer JC, Krill CE,
Johnson WL. Structural and
thermodynamic properties of
nanocrystalline fcc metals prepared
by mechanical attrition. Journal of
Materials Research. 1992;**7**(7):1751-1761.
DOI: 10.1557/JMR.1992.1751